EPJ Web of Conferences **145**, 04002 (2017) DOI: 10.1051/epjconf/201714504002
ISVHECRI 2016

Particle acceleration in binaries

V.G. Sinitsyna[a] and V.Y. Sinitsyna

P. N. Lebedev Physical Institute, Russian Academy of Science, Russia

Abstract. Cygnus X-3 massive binary system is one of the powerful sources of radio and X-ray emission consisting of an accreting compact object, probably a black hole, with a Wolf-Rayet star companion. Based on the detections of ultra high energy gamma-rays by Kiel and Havera Park, Cygnus X-3 has been proposed to be one of the most powerful sources of charged cosmic ray particles in the Galaxy. The results of long-term observations of the Cyg X-3 binary at energies 800 GeV–85 TeV detected by SHALON in 1995 are presented with images, integral spectra and spectral energy distribution. The identification of source with Cygnus X-3 detected by SHALON was secured by the detection of its 4.8 hour orbital period in TeV gamma-rays. During the whole observation period of Cyg X-3 with SHALON significant flux increases were detected at energies above 0.8 TeV. These TeV flux increases are correlated with flaring activity at a lower energy range of X-ray and/or at observations of Fermi LAT as well as with radio emission from the relativistic jets of Cygnus X-3. The variability of very high-energy gamma-radiation and correlation of radiation activity in the wide energy range can provide essential information on particle mechanism production up to very high energies. Whereas, modulation of very high energy emission connected to the orbital motion of the binary system, provides an understanding of the emission processes, nature and location of particle acceleration.

1. Introduction

SHALON is a high-altitude imaging atmospheric Cherenkov telescope for the detection of very high energy γ-rays from 800 GeV to 100 TeV. γ-astronomical research has been carryied out with the SHALON telescope since 1992. During the period 1992–2016 SHALON has been used for observations of different galactic and extragalactic objects (see these Proceedings and [1]). Among them are objects of the Cygnus region.

The Cygnus region contains a number of sources of radio and X-ray emission and some of them were detected at high energies. The most powerful have also been supposed to be GeV-TeV γ-ray emitters. Among them are the Cyg X-3 massive binary system (Figs. 1, 2, 3, 4, 5, 6, 7).

2. SHALON mirror Cherenkov telescopes

The SHALON γ-ray telescopes are located at an altitude of 3340 m above sea level each of which has a composite mirror with an area of 11.2 m^2. The detector array consisting of 144 FEU-85 photomultipliers assembled into a square array and mounted at the mirror focus has characteristics sufficient to record information about the shower structure in the energy range under consideration. The detector has the largest field of view in the world, $> 8^\circ$. This allows one to monitor the background from charged cosmic-ray particles and the atmospheric transparency continuously during observations and expands the area of observation and, hence, the efficiency of observations [2]. The technique for simultaneously obtaining information about the cosmic-ray background and the showers initiated by γ-rays is unique and has been applied in the SHALON experiment from the very beginning of its operation [2]. This technique serves to increase the useful source tracking time and, what is particularly important, such source and background observation conditions as the thickness and state of the atmosphere remain the same. In addition, the wide field of view allows recording the off-center showers arriving at distances of more than 30 m from the telescope axis completely and almost without any distortions; they account for more than 90% of all the showers recorded by the telescope.

Due to criteria used in our experiment the background is rejected with 99.92% efficiency and the amount of background gamma-like events is less than 10%. During a primary analysis, the primary particle arrival direction is determined with an accuracy up to $\leq 0.1^\circ$. The subsequent analysis specially developed for the SHALON telescopes and based on the Tikhonov regularization method [3,4] improves the accuracy to a value of less than 0.01° [5].

3. Cygnus X-3

The binary system Cyg X-3 is one of the brightest Galactic X-ray sources, displaying high and low states and rapid variability in X-rays. In addition to being a powerful X-ray source, Cyg X-3 is seen in the infrared and is a strong and variable radio source. It is also the strongest radio source among X-ray binaries (Fig. 1) and shows both huge radio outbursts and relativistic jets. The radio-activity is closely linked with the X-ray emission and the different X-ray states [7,8]. Cygnus X-3 is a high mass X-ray binary and microquasar, with a compact object, which is either a neutron star or may be a black hole, and a companion

[a] e-mail: sinits@sci.lebedev.ru

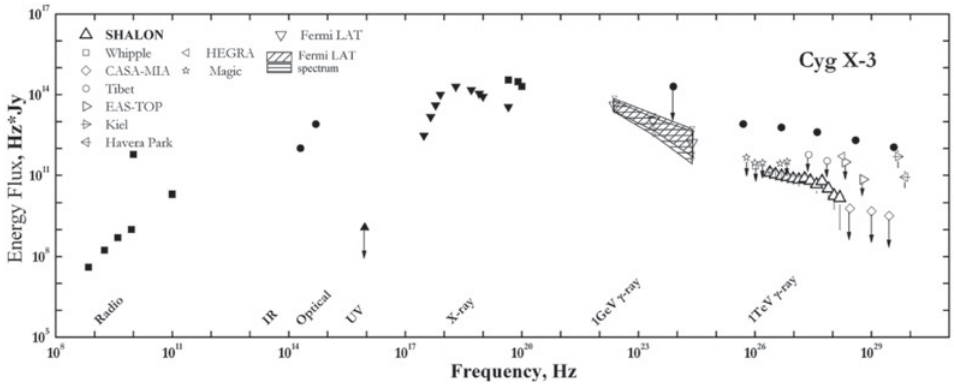

Figure 1. Spectral energy distribution of γ-ray emission from Cyg X-3. △ represent the data from the SHALON Cherenkov telescope. Black points are the archival data from [6].

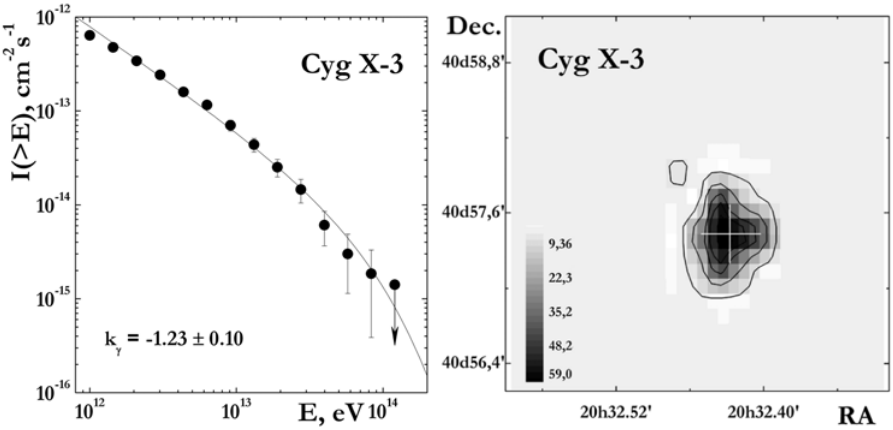

Figure 2. Left: the γ-ray integral spectra of Cyg X-3 averaged over the period 1995–2015. Right: TeV γ-ray emission map of Cyg X-3.

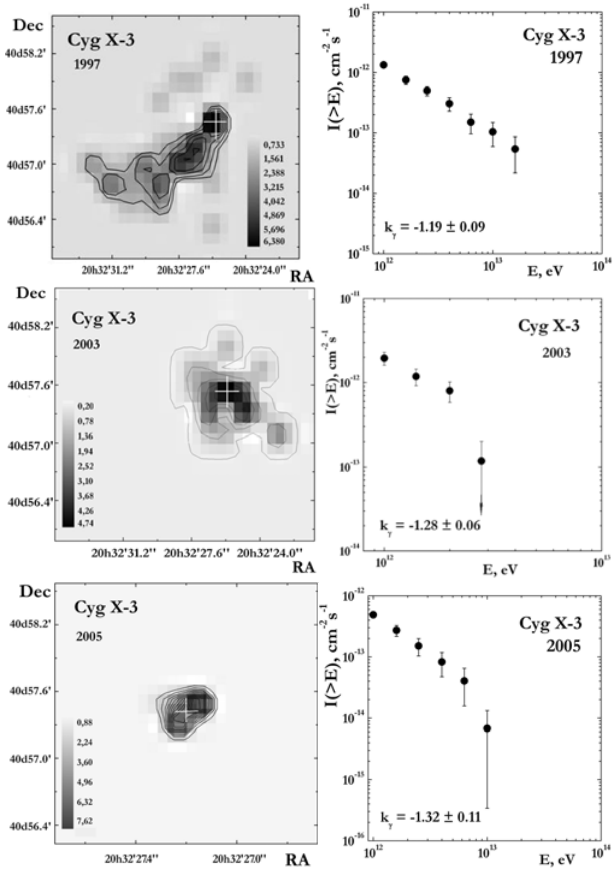

Figure 3. Left: the image of γ-ray emission from Cyg X-3 in 1997, 2003 and 2005 by SHALON; Right: the γ-ray integral spectra with the power index k_γ.

object, which is a Wolf-Rayet star. But Cygnus X-3 shows a short orbital period of 4.8 hours, typical of low mass binaries. It has been inferred from the modulation of both X-ray (Fig. 6) and infrared emissions. The nature of the compact object is still uncertain. Based on the detections of ultra high energy γ-rays [9,10], Cygnus X-3 has been proposed to be one of the most powerful sources of charged cosmic ray particles in the Galaxy (Fig. 1).

Attempts to detect TeV emission from Cygnus X-3 were first made in the mid 1970s and continued through the mid 1980s. Two observations were particulary important: the Kiel [9] results and contemporaneous observations at Haverah Park [10]. These results indicated a very large UHE flux from Cygnus X-3. So, these results stimulated the construction of many new detectors. The upper limits of the Cygnus X-3 flux are over an order of magnitude lower than detected in the 1980s. Figure 1 also shows upper limits on the steady flux from Cygnus X-3 reported between 1990 and 1995 compared with earlier observations.

4. Cyg X-3 viewed in TeV gamma-rays

Cyg X-3 has been regularly observed since 1995 with the SHALON telescope [2] during a total of 303.2 hours. The observations were performed using the standard (for SHALON) technique of obtaining information about the cosmic-ray background and γ-ray-initiated showers in the same observing session. The SHALON method of selecting γ-ray showers from background cosmic-ray showers allows to reject 99.92% of the background showers [1]. The γ-ray source associated with Cyg

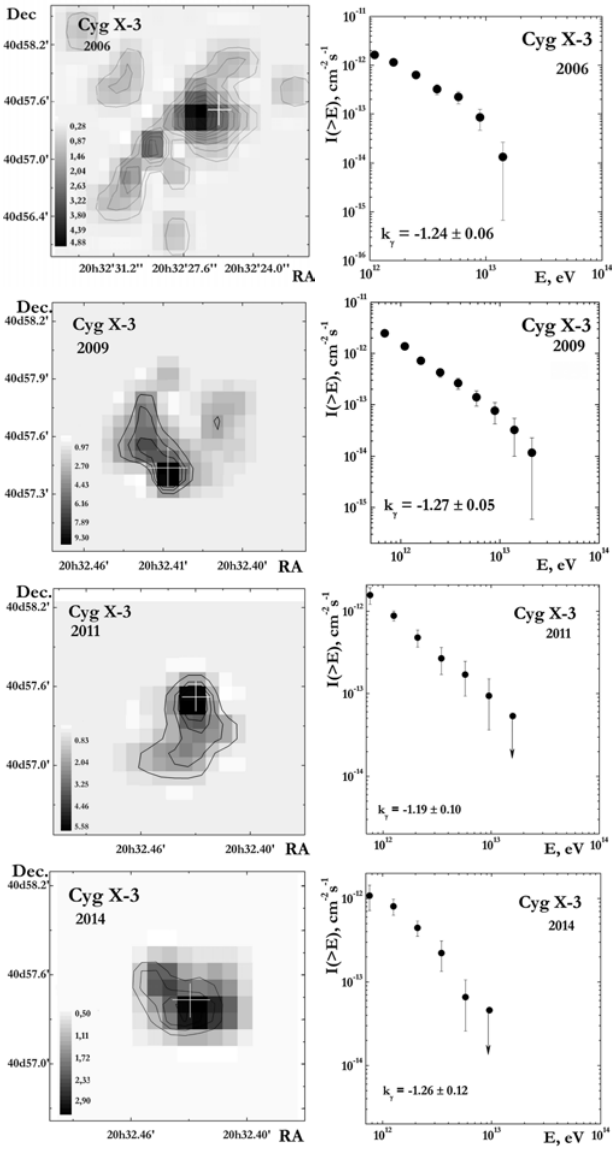

Figure 4. Left: the image of γ-ray emission from Cyg X-3 in 2006, 2009, 2011 and 2014 by SHALON; Right: the γ-ray integral spectra with the power index k_γ.

X-3 was detected above 800 GeV with a statistical significance [11] of 41.2σ with a average integral γ-ray flux above 800 GeV $F(E_\circ > 0.8\,\mathrm{TeV}) = (6.8 \pm 0.4) \times 10^{-13}\,\mathrm{cm}^{-2}\,\mathrm{s}^{-1}$ [12–16]. The energy spectrum of Cyg X-3 at 800 GeV–85 TeV can be approximated by the power law $F(> E_O) \propto E^{-1.23\pm0.10}$. Also, the γ-ray energy spectrum of Cyg X-3 can be fitted by a power law with an exponential cutoff $I(> E_\gamma) = (0.68 \pm 0.04) \times 10^{-12} \times E^{-1.15\pm0.08} \times \exp(-E_\gamma/75\,\mathrm{TeV})\,\mathrm{cm}^{-2}\,\mathrm{s}^{-1}$ (see Fig. 2). In Fig. 2, right TeV emission region in energy range of 0.8–100 TeV during the whole period of SHALON observations of Cyg X-3 is shown.

5. Flaring activity of Cyg X-3

Extreme variability in different wavelengths including VHE γ-rays is the remarkable feature of Cyg X-3 (Fig. 5). A number of high activity periods of Cyg X-3 were detected with SHALON at energies > 800 GeV during the whole period of observation since 1995. In the last 10 years Cyg X-3 has shown activity in all wavelengths. Some results on TeV activity detected by SHALON are presented in (Figs. 3, 4).

The binary Cyg X-3 came to a period of flaring activity at radio-and X-ray energies in 2006 (Fig. 4). In May and July 2006 a significant increase of the Cyg X-3 flux was detected with SHALON at TeV energies with flux values $(4.12 \pm 1.01) \times 10^{-12}\,\mathrm{cm}^{-2}\,\mathrm{s}^{-1}$ and $(1.62 \pm 0.75) \times 10^{-12}\,\mathrm{cm}^{-2}\,\mathrm{s}^{-1}$ respectively. The γ-ray flux in June $(0.46 \pm 0.18) \times 10^{-12}\,\mathrm{cm}^{-2}\,\mathrm{s}^{-1}$ [16].

The average γ-ray flux detected by SHALON in the flaring period from May to July 2006 was estimated as $(1.47 \pm 0.24) \times 10^{-12}\,\mathrm{cm}^{-2}\,\mathrm{s}^{-1}$ (Fig. 4). This intensity increase was also observed by the Crimea Observatory and the integral flux was estimated to be $F(E_\circ > 1\,\mathrm{TeV}) \sim (3\text{–}5) \times 10^{-12}\,\mathrm{cm}^{-2}\,\mathrm{s}^{-1}$. [17].

Cyg X-3 was in a quiet period at TeV energies in 2005. The average γ-quantum flux from Cyg X-3 for $E > 0.8$ TeV is estimated to be $F(E_O > 0.8\,\mathrm{TeV}) = (5.4 \pm 0.73) \times 10^{-13}\,\mathrm{cm}^{-2}\,\mathrm{s}^{-1}$ (Fig. 3). The images and spectra of Cyg X-3 in the 2005 silent period are shown in Fig. 3. No features revealed during flaring periods were found.

The γ-ray flux detected by SHALON in 2003 was estimated as $(1.79 \pm 0.33) \times 10^{-12}\,\mathrm{cm}^{-2}\,\mathrm{s}^{-1}$ (Fig. 3). Earlier, in 1997, a comparable increase of the flux over the average value was also observed and estimated to be $(1.2 \pm 0.5) \pm 10^{-12}\,\mathrm{cm}^{-2}\,\mathrm{s}^{-1}$ (Fig. 3).

The last significant increase of very high energy γ-quantum flux was detected in May 2009: $(3.1 \pm 0.98) \times 10^{-12}\,\mathrm{cm}^{-2}\,\mathrm{s}^{-1}$ (Fig. 4). The increase is correlated with the flaring activity at a lower X-ray energy range and with observations of Fermi LAT [18,19] with average flaring flux of $F = (190 \pm 40) \times 10^{-8}\,\mathrm{phcm}^{-2}\,\mathrm{s}^{-1}$ above 100 MeV (Fig. 5). In the autumn of 2009 Cyg X-3 comes again to a quiet period at TeV energies. The average γ-quantum flux from Cyg X-3 for energies above 0.8 TeV is estimated to be $(0.46 \pm 0.07) \times 10^{-12}\,\mathrm{cm}^{-2}\,\mathrm{s}^{-1}$ with $k_\gamma = -1.10 \pm 0.12$. No significant change of spectrum index was observed in total between high and low states of Cyg X-3.

The last increases of very high energy γ-ray flux were detected in October 2011 and 2014, which were correlated with flaring activity at lower energy range of soft X-ray and/or by observations of Fermi LAT [19]. A high TeV γ-ray flux was detected by SHALON during the X-ray flares of end-September and mid-October 2014 observed by MAXI [20]. Images and spectra of TeV emission are presented in Fig. 4.

Reliably revealing flares and their duration in long-term observations with mirror Cherenkov telescopes is complicated by the fact that the technique makes a continuous tracking of the source impossible, because it requires such conditions as moonless nights, which already creates a gap in the data for more than 10 days; an ideal atmosphere without clouds and haze and, in addition, the source's passage at a distance of no more than 35° from the zenith are needed, because the influence of a change in atmospheric thickness should be minimal.

Nevertheless, revealing correlations between the emissions in different energy ranges, comparing the emission regions, and, in particular, the detection of the flux changes remains necessary, because it makes it possible to judge the nature of the source, namely Cyg X-3, its evolution, and the emission generation mechanisms.

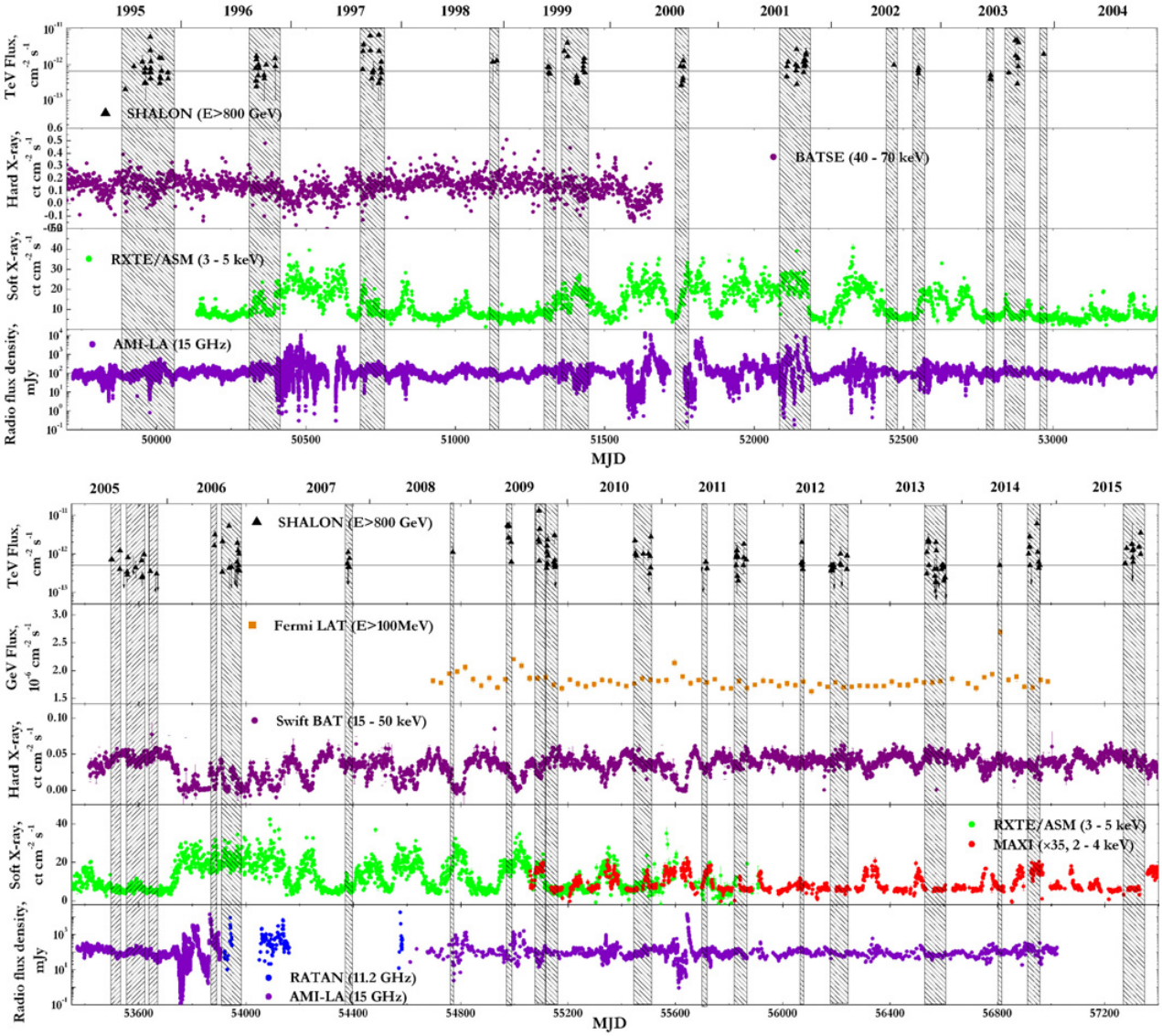

Figure 5. The light curves of Cyg X-3 in a wide energy range.

To reveal possible correlation of periods of activity in the TeV energy range with the flares at the low energies the light curves of Swift/BAT (15–50 keV)[1], MAXI (2–4 keV) [20], RXTE/ASM (3–5 keV)[2], the fluxes at radio-ranges from RATAN (11.2 GHz) (see [21]), AMI-LA (15 GHz)[3] and TeV fluxes from SHALON observations were analyzed (Fig. 5). Analysis of the Cyg X-3 light curve obtained by SHALON shows that the intervals of low flux at TeV energies are at the low activity periods of radio and soft X-rays, but at high flux periods at hard X-rays. There are three type of low energy Cyg X-3 behavior when TeV gamma-ray flares appear.

Cyg X-3 flares at energies >0.8 TeV, detected by SHALON, occur in the case of the intermediate radio flare (< 1000 mJy) at the sharp radio-flux fall before the increase (7–15 days before the radio-flare, as in 1995, 1997, 1999 years). And a very high energy increased flux was detected during the decay period in soft X-rays some 6–8 days after the maximum.

A TeV gamma-ray flux increase appears simultaneously with the main radio-flare (>1000 mJy) at the period of high level flux in soft X-rays (2001).

It was also found that TeV flares occur at the period of high flux of soft X-rays and low activity of hard X-rays within the 5–8 days before the intermediate and main radio flare (2006, 2009) and 7–15 days after the main radio-flare (2006).

The duration of the increase of the detected TeV-flare is from 1 to 4 days andthe duration of fall is 1 day.

A correlation of TeV and soft X-ray fluxes was found in the 1997 observation period. But the flux increase of 2003 didn't obey this scheme, it was in the quiet period of the soft X-rays. In general, the correlation of soft X-ray and TeV energy γ-ray fluxes is traced since 1996.

During the period of observations of Cyg X-3 with SHALON 8, significant flux increases were detected at energies above 0.8 TeV. The significant anti-correlation of the fluxes at TeV and hard X-rays and the correlation of very high energy flux and soft X-ray were found. It is

[1] `http://swift.gsfc.nasa.gov/results/transients/CygX-3/`
[2] `http://xte.mit.edu/asmlc/srcs/cygx3.html`
[3] `http://www.mrao.cam.ac.uk/ guy/cx3/`

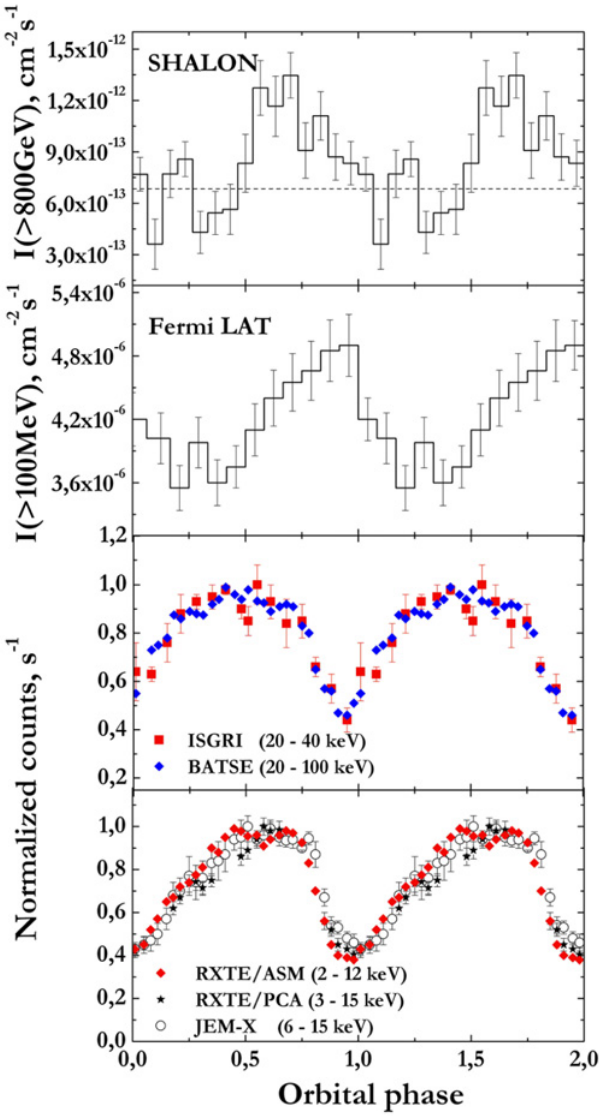

Figure 6. SHALON, Fermi LAT [19] and X-ray light curves of Cyg X-3 folded on the orbital period; The dashed line shows the level of averaged integral TeV γ-ray flux by SHALON.

noted, that TeV flaring activities occur within 5–8 days of strong radio flares (Fig. 5). It is probably, linked with the powerful ejection from the regions close to the centers blackhole. This ejection is accompanied with a relativistic shock where the relativistic electrons and magnetic field are effectively generated.

6. Orbital period

To securely identify the detected emission with Cyg X-3, a timing analysis to search for the 4.8-hour orbital period of Cyg X-3 was performed (see. Fig. 6). We compared the SHALON light curve folded on the orbital period to the folded >100 MeV light curve of Cyg X-3 from Fermi LAT together with X-ray data by RXTE/ASM (2–12 keV), RXTE/PCA (3–15 keV), JEM-X (6–15 keV) and ISGRI (20–40 keV), BATSE (20–100 keV).

The folded X-ray, GeV and TeV light curves have a similar asymmetric shape with a slow rise followed by a faster decay. Also, the SHALON and Fermi LAT light curves are shifted by about 0.15 in phase and its shape have the local maxima. But the phase of the SHALON minimum flux is close to the phase of the minimum of the soft X-ray count rate, shifted by 0.3 in phase (Fig. 6). The observed modulation of high and very high energy gamma-rays suggests that the emission region size and location are bounded by the system size.

7. Phase-resolved energy spectra

The determination of the energy spectrum of very high energy emission is important for understanding the mechanism of radiation production. In the case of the binaries the phase resolved spectra, especially if they vary with phase, can bring information about the generation mechanism of TeV gamma-rays and point out the site of origin.

Spectra of three intervals of orbital phase of Cyg X-3 binary system were extracted.

1. The interval with maximum flux corresponding to inferior conjunction at phase $0.0 \leq \phi < 0.05$; $0.45 \leq \phi < 1.0$; The γ-ray energy spectrum is well described by a relatively soft power law with an exponential cutoff:
   $I(> E_\gamma) = (1.5 \pm 0.4) \times 10^{-12} \times E^{-1.15\pm0.10} \times \exp(-E_\gamma/20\,\mathrm{TeV})\,\mathrm{cm}^{-2}\,\mathrm{s}^{-1}$
   (see black points in Fig. 7)
2. The interval with additional maximum at the epoch of superior conjunction at phase $0.12 \leq \phi < 0.25$; The γ-ray energy spectrum is described by a hard power law:
   $I(> E_\gamma) = (0.67 \pm 0.10) \times 10^{-12} \times E^{-0.93\pm0.09}\,\mathrm{cm}^{-2}\,\mathrm{s}^{-1}$
   (see open triangles in Fig. 7)
3. The interval with minimum flux corresponding to superior conjunction at phase $0.05 \leq \phi < 0.12$; $0.25 \leq \phi \leq 0.45$; Here the γ-ray energy spectrum is described by a hard power law with an exponential cutoff:
   $I(> E_\gamma) = (0.4 \pm 0.08) \times 10^{-12} \times E^{-0.70\pm0.09} \times \exp(-E_\gamma/14.5\,\mathrm{TeV})\,\mathrm{cm}^{-2}\,\mathrm{s}^{-1}$
   (see open squares in Fig. 7).

Inverse Compton (IC) scattering of photons from the WR star on very high energy electrons is a natural candidate to explain the TeV gamma-ray emission. IC scattering directly produces a modulation of the flux because of the orbital motion. The maximum occurs when stellar photons are backscattered towards the observer (inferior conjunction). The observed connection between gamma-ray and radio flares suggests that the high energy electrons are located in the relativistic jet and situated in two symmetric locations in a relativistic jet. The detection of gamma-rays in the phases corresponding to additional maximum at superior conjunction in the large energy range of 800 GeV–100 TeV with hard energy spectrum in whole interval without the presence of a cutoff is argued in favor of the hadronic origin of these energetic photons.

8. Conclusion

The Cygnus Region contains a number of powerful sources of radio and X-rays which are supposed to be potential TeV-emitting objects. The results of 20-year observations of Cyg X-3 at energies 0.8–85 TeV, first detected by

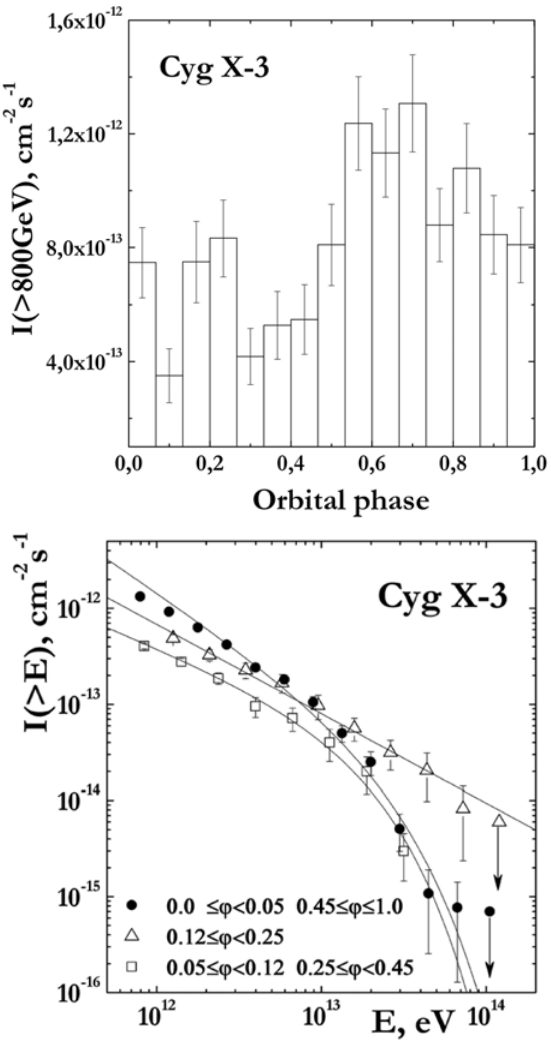

Figure 7. Top: SHALON light curves of Cyg X-3 folded on the orbital period; Bottom: phase-resolved energy spectra by SHALON (see text).

the SHALON telescope in 1995, are presented. The identification of a source associated with Cygnus X-3, detected by SHALON, was secured by the detection of its 4.8 hour orbital period in TeV gamma-rays. A number of high activity periods of Cyg X-3 were detected by SHALON during the whole period of observation. The significant increases of flux are correlated with flaring activity at the lower energy range of X-ray and/or at observations of Fermi LAT. The detected modulation of very high energy emission connected to the orbital motion of the binary system, provides understanding of the emission processes, nature and location of particle acceleration.

References

[1] V.G. Sinitsyna, V.Yu. Sinitsyna, Astron. Lett. **37**(9), 621 (2011)
[2] V.G. Sinitsyna, Nuovo Cim. **19C**, 965 (1996)
[3] A.N. Tikhonov, V.Ya. Arsenin, *Solutions of Ill-Posed Problems* (Nauka, Moscow, 1979; Halsted, New York, 1977)
[4] A.V. Goncharskii et al., *Ill-Posed Problems in Astrophysics* (Nauka, Fizmatlit, Moscow, 1985)
[5] V.G. Sinitsyna, V.Yu. Sinitsyna, Astron. Lett. **40**(2–3), 75 (2014)
[6] F.A.-D. Cordova, Los Alamos Science, Spring, 39 (1986)
[7] M.L. Mccollough et al., Astrophys. J. **517**, 951 (1999)
[8] S.A. Trushkin et al., Proc. of IAU Symposium No. 238, 2006 (ed V. Karas, G. Matt), p. 463
[9] M. Samorscki, W. Stamm, Astrophys. J. **268**, L17 (1983)
[10] J. Lloyd-Evans et al., Nature **305**, 784 (1983)
[11] T.-P. Li and Y.-Q. Ma, Astrophys. J. **272**, 317 (1983) 317
[12] V.G. Sinitsyna, AIP **515**, 205, 293 (2000)
[13] V.G. Sinitsyna et al., Int. J. Mod. Phys. A **29**, 7023 (2005)
[14] V.G. Sinitsyna, Rad. Phys. and Chem. **75**, 880 (2006)
[15] V.G. Sinitsyna et al., J. Phys. Soc. Jpn., Suppl. A **78**, 92 (2009)
[16] V.G. Sinitsyna, V.Yu. Sinitsyna, *"Cosmic Rays For Particle And Astroparticle Physics"* (Proc. 12th ICATPP, 2010) ed S. Giani, C. Leroy, and P.G. Rancoita; (Singapore: World Scientific 2011) vol. 6, p. 132
[17] Yu.T. Neshpor et al., Bull. of RAS; Physics **73**(5), 694 (2009)
[18] M. Tavani et al., Nature Letters **462/3**, 620 (2009)
[19] A.A. Abdo et al., Science **326**, 1512 (2009)
[20] M. Matsuoka et al., PASJ **61**, 999 (2009)
[21] J. Alekśic et al., Astrophys. J. **721**, 843 (2010)